Folded acoustic phonons in GaAs/AlAs corrugated superlattices grown along the [311] direction

Z. V. Popović, J. Spitzer, T. Ruf, M. Cardona, R. Nötzel, and K. Ploog*

Max-Planck-Institut für Festkörperforschung, Heisenbergstraße 1, 70569 Stuttgart 80, Federal Republic of Germany

We present Raman spectra for folded acoustic phonons in GaAs/AlAs superlattices grown along the [311] direction. The symmetry of this direction offers the rare possibility of observing folded phonons of all three acoustic branches. In accordance with the predicted selection rules the Raman spectra show doublets of modes of pure transverse (polarized along the [0$\bar{1}$1] direction) as well as mixed transverse and longitudinal character. The frequencies and strengths of these modes are also in agreement with calculations based on the continuum model. Folded-phonon to Brillouin ratios are calculated using elasto-optic constants of GaP in lieu of AlAs.

I. INTRODUCTION

Superlattices have to date been mainly grown on (001)-oriented GaAs substrates on the assumption that this guarantees high structural quality. Recently it has been reported[1-4] that high-quality superlattices can be grown by molecular-beam epitaxy (MBE) practically on any low-index crystallographic plane: (hkl), for h, k, l = 0, 1, 2. Moreover, it has been shown that quantum wells and superlattices grown in other directions, e.g., [111], may have interesting properties.[5] Quantum structures on (311)-oriented GaAs substrates have attracted special attention because of the direct synthesis of GaAs quantum-wire structures due to the *in situ* formation of an array of nanometer-scale macrosteps or facets with a periodicity determined by energy, rather than growth-related parameters.[6] The (311) surface is particularly interesting because, depending on the growth conditions, Si can either incorporate into Ga or into As sites, acting therefore either as a donor or an acceptor.[7] This suggests that semiconducting devices could be fabricated by all-silicon doping.

Raman scattering by folded acoustic phonons in semiconductor superlattices (SL) has generated increasing interest in the last few years. Most reported measurements were performed on (001)-oriented GaAs/AlAs superlattices in which only the longitudinal acoustic (LA) branch is Raman active in backscattering (for a review, see, e.g., Ref. 8). For (110)- and (111)-oriented GaAs/AlAs superlattices only folded phonons from the longitudinal acoustic branch have been observed.[2,3] The first report of scattering by transverse folded acoustic phonons (TA) involved (012)-oriented GaAs/AlAs superlattices.[9]

In this paper we present Raman scattering spectra by folded acoustic phonons in a series of (311)-oriented GaAs/AlAs superlattices and demonstrate that folded phonons of all three acoustic branches are observed. Their frequencies and intensities are in good agreement with continuum model calculations. Folded-phonon to

Brillouin scattering ratios compare favorably with those predicted by using the elasto-optic constants of the electronically similar GaP instead of AlAs, for which these parameters are not known.

II. EXPERIMENT

We studied five GaAs/AlAs superlattices with a period between d = 46 Å and d = 127 Å. They were grown by MBE on (311)-oriented, undoped, semi-insulating GaAs substrates. Details of the growth procedure and the x-ray characterization have been given earlier.[6,10] To illustrate the sample quality, Fig. 1 shows the x-ray-diffraction pattern for one of these superlattices. This pattern was recorded in the vicinity of the (311) GaAs reflection by using a double-crystal x-ray diffractometer. The diffrac-
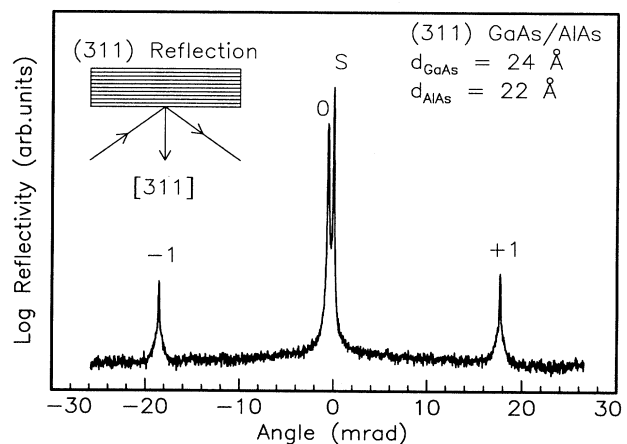

FIG. 1. X-ray-diffraction pattern of the (24/22)-Å superlattice, measured with the Cu $K\alpha_1$ line (λ = 1.540 56 Å) in the vincinity of the (311) reflection. S denotes the GaAs substrate peak, 0 and ± 1 the superlattice peaks.

48   1659

tion geometry is shown in the inset of Fig. 1. The corresponding diffraction pattern exhibits a main superlattice peak (0) close to the GaAs substrate peak (S). The angular distance between the superlattice peak and the substrate peak is related to the ratio between the GaAs and AlAs layer thicknesses. The sharp and distinct first-order satellite peaks (labeled $+1$ and -1 in Fig. 1) are observed for all samples and demonstrate the high structural quality. The angular separation of those peaks gives the superlattice period length. The total thickness of the superlattices is ≈ 0.7 μm, the thicknesses of the individual GaAs and AlAs layers are (in Å) $(d_{\text{GaAs}}, d_{\text{AlAs}})$ $= (24, 22)$, $(29, 29)$, $(43, 47)$, $(56, 50)$, and $(66, 61)$, a monolayer of the (311) superlattices being ≈ 1.7 Å . Therefore, these values correspond to $(n, m) = (14, 13)$, $(17, 17)$, $(25, 28)$, $(33, 29)$, and $(39, 36)$ monolayers.

The Raman spectra were recorded in quasibackscattering geometry, using a Spex Industries 1-m double monochromator with 1800-grooves/mm holographic gratings and conventional photon counting techniques. For the large-period samples we used a SOPRA 2.12-m double monochromator. The 4579-, 4880-, and 5145-

Å lines of an Ar$^+$-ion laser with an average power of 100 mW focused to a line were employed as excitation sources with the samples kept in vacuum at room temperature.

III. RESULTS AND DISCUSSION

The propagation properties of acoustic waves in a superlattice can be obtained from the propagation of acoustic waves in the parent materials.[8] For cubic solids (e.g., GaAs), there are three directions of propagation ($\langle 100 \rangle$, $\langle 110 \rangle$, and $\langle 111 \rangle$) along which the long-wavelength acoustic waves are purely longitudinal and transverse in character (in the $\langle 110 \rangle$ case only for small q, i.e., within the elastic approximation). Along the [311] direction, there is only one pure transverse mode (polarized along the [0$\bar{1}$1] direction) and the other two modes have mixed longitudinal and transverse character. The velocities of these waves can be calculated using the Christoffel equation.[11] In the case of the [311] growth direction they are obtained by solving the secular equation,

$$\begin{vmatrix} 9c_{11} + 2c_{44} - 11\rho\omega^2/k^2 & 3\left(c_{12} + c_{44}\right) & 3\left(c_{12} + c_{44}\right) \\ 3\left(c_{12} + c_{44}\right) & c_{11} + 10c_{44} - 11\rho\omega^2/k^2 & \left(c_{12} + c_{44}\right) \\ 3\left(c_{12} + c_{44}\right) & \left(c_{12} + c_{44}\right) & c_{11} + 10c_{44} - 11\rho\omega^2/k^2 \end{vmatrix} = 0 \tag{1}$$

where c_{ij} are the elastic constants and ρ is the mass density. The values of the velocities for the [311] direction obtained from Eq. (1), are

$$v_T^2 = \left(c_{11} - c_{12} + 9c_{44}\right)/11\rho, \tag{2}$$

$$v_{\text{QT}}^2 = \left(10c_{11} + c_{12} + 13c_{44} - D\right)/22\rho, \tag{3}$$

$$v_{\text{QL}}^2 = \left(10c_{11} + c_{12} + 13c_{44} + D\right)/22\rho \tag{4}$$

with

$$D = \left[\left(8c_{11} - c_{12} - 9c_{44}\right)^2 + 72\left(c_{12} + c_{44}\right)^2\right]^{1/2} .$$

Equation (2) yields the velocity of a pure transverse (T) wave polarized along the [0$\bar{1}$1] axis. Equations (3) and (4) describe quasitransverse (QT) and quasilongitudinal (QL) waves, respectively. Using the tabulated elastic constants of GaAs and AlAs,[12] we calculated the acoustic velocities for the [311] propagation direction (see Table I).

The Raman selection rules for the folded acoustic phonons of superlattices in the elastic approximation can be extracted from the Brillouin tensors of the corresponding bulk crystals.[8] For $q = [311]/\sqrt{11}$ the acoustic phonon-modulated (Brillouin) dielectric tensors R^j are

$$\frac{\epsilon_0^2}{\sqrt{22}}\begin{pmatrix} 0 & -3p_{44} & 3p_{44} \\ -3p_{44} & p_{12} - p_{11} & 0 \\ 3p_{44} & 0 & p_{11} - p_{12} \end{pmatrix} \quad \text{for the } T^{[0\bar{1}1]} \text{ mode,} \tag{5}$$

$$\frac{\epsilon_0^2}{11\sqrt{2}}\begin{pmatrix} -9p_{11} + 4p_{12} & 3p_{44} & 3p_{44} \\ 3p_{44} & -7p_{12} + 2p_{11} & 4p_{44} \\ 3p_{44} & 4p_{44} & -7p_{12} + 2p_{11} \end{pmatrix} \text{ for the } \text{QT}^{[2\bar{3}3]} \text{ mode,} \tag{6}$$

$$\frac{\epsilon_0^2}{11}\begin{pmatrix} 9p_{11} + 2p_{12} & 6p_{44} & 6p_{44} \\ 6p_{44} & p_{11} + 10p_{12} & 2p_{44} \\ 6p_{44} & 2p_{44} & p_{11} + 10p_{12} \end{pmatrix} \quad \text{for the } \text{QL}^{[311]} \text{ mode,} \tag{7}$$

TABLE I. Velocities of the three acoustic modes for GaAs and AlAs for propagation along [311], obtained using the elastic constants (in GPa) listed in Ref. 12: $c_{11} = 119$, $c_{12} = 53.8$, and $c_{44} = 59.5$ for GaAs, and $c_{11} = 120.2$, $c_{12} = 57.0$, and $c_{44} = 58.9$ for AlAs.

Acoustic mode	v (10^5 cm/s)	
	GaAs	AlAs
T	3.2	3.79
QT	2.91	3.43
QL	5.1	6.1

where p_{ij} are the elasto-optic (or photoelastic) constants. We have used these tensors to determine the selection rules for folded acoustic phonons given in Table II. The linear combinations of elasto-optic constants which contribute to the scattering in the different polarization geometries of Table II are

$$a = (2p_{11} - 7p_{12} - 4p_{44})\, \epsilon_0^2/11\sqrt{2},$$
$$b = (p_{11} + 10p_{12} - 2p_{44})\, \epsilon_0^2/11,$$
$$c = (p_{11} - p_{12} - 2p_{44})\, 3\epsilon_0^2/11\sqrt{2}, \qquad (8)$$
$$d = 5\epsilon_0^2 p_{12}/11\sqrt{2},$$
$$e = (27p_{11} + 94p_{12} - 54p_{44})\, \epsilon_0^2/121.$$

According to the selection rules folded phonons from all three acoustic dispersion branches are optically active. Therefore, superlattices grown along the [311] direction allow the study of both pure and mixed transverse folded acoustic modes. The quasitransverse folded acoustic phonons, polarized approximately along [$\bar{2}33$], may be observed in parallel polarizations, whereas the [$0\bar{1}1$] transverse polarized phonons are allowed in crossed polarizations.

Raman scattering spectra for the (311)-oriented (24,22)-Å superlattice in the spectral range between -50 cm^{-1} and 50 cm^{-1} are shown in Fig. 2(a). The laser line of 4579 Å corresponds to nonresonant conditions. In agreement with the selection rules given in Table II, for $z(x'x')\bar{z}$ and $z(y'y')\bar{z}$ polarizations the QT- and QL-folded acoustic-phonon doublets are clearly observed. For crossed polarizations [$z(x'y')\bar{z}$], only a pure transverse (T) acoustic-phonon doublet appears strongly. The frequencies of these modes are shifted from the QT doublets by about 1.5 cm^{-1}, in agreement with the velocity

TABLE II. The polarization selection rules in backscattering geometry for the folded acoustic phonons of GaAs/AlAs superlattices grown along the [311] direction, as carried over from those of the bulk crystal. a-e are elasto-optic tensor components as described in the text.

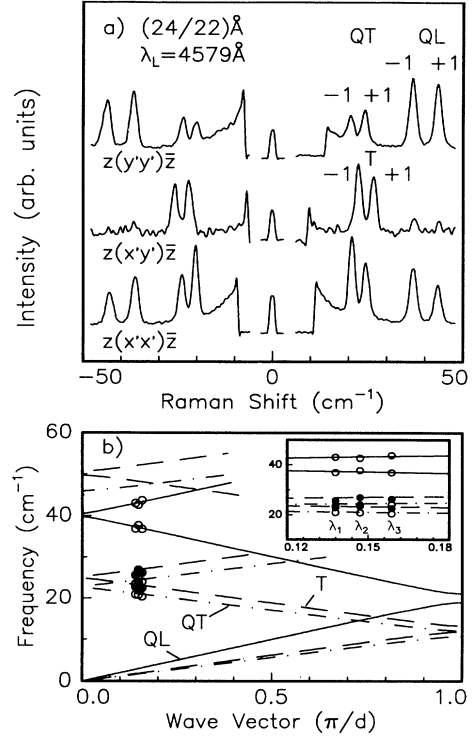|	Polarization		Scattering cross section		
Configuration	Incident	Scattering	$T^{[0\bar{1}1]}$	QT$^{[\bar{2}33]}$	QL$^{[311]}$
$z(x'x')\bar{z}$	[$0\bar{1}1$]	[$0\bar{1}1$]	0	a^2	b^2
$z(x'y')\bar{z}$	[$0\bar{1}1$]	[$\bar{2}33$]	c^2	0	0
$z(y'y')\bar{z}$	[$\bar{2}33$]	[$\bar{2}33$]	0	d^2	e^2

FIG. 2. (a) Stokes and anti-Stokes Raman scattering spectra of the (24/22)-Å superlattice, measured at $T = 300$ K with an excitation wavelength of 4579 Å in three different polarizations. QT denotes the quasitransverse, QL the quasilongitudinal, and T the pure transverse mode. (b) Comparison of the measured phonon frequencies with the continuum model, using the velocity values of Table I. o: $z(x'x')\bar{z}$, •: $z(x'y')\bar{z}$. The inset shows the phonon frequencies measured with different excitation wavelengths ($\lambda_1 = 5145$ Å, $\lambda_2 = 4880$ Å, $\lambda_3 = 4579$ Å).

differences between v_T and v_{QT} (see Table I). In addition to the T doublet there are much weaker modes in the $z(x'y')\bar{z}$ polarizations at about 37 and 44 cm^{-1}. We assign these modes to a QL doublet because the frequencies correspond to those of the QL doublet observed for parallel polarizations. These modes are actually forbidden by the selection rules, but may be observed because of a possible leakage of polarization or deviations from the nominal superlattice geometry.

The asymmetry of the intensities observed for the two peaks is the same for the T, QT, and QL doublets. This can be understood on the basis of the intensity analysis of folded phonons in (001) GaAs/AlAs superlattices (see Fig. 3.26 of Ref. 8). For the superlattices studied here, the parameter $\alpha = (d_{\text{AlAs}}/d_{\text{GaAs+AlAs}})$ is between 0.48 and 0.52. For these values of α the -1 line should be stronger than the $+1$ line, and the intensities of the second folded T, QT, and QL doublets should be small. It is interesting to note that the difference in frequency between the doublet peaks [Fig. 2(a)] is $\Delta\omega = 4.0$, 3.7, and 6.6 cm^{-1} for T, QT, and QL folded phonons, respectively. According to the doublet splitting, described

for large wavelengths in terms of the superlattice sound velocity v_{SL} by[13]

$$\Delta\omega = v_{SL}\frac{8\pi n}{\lambda_L},\qquad(9)$$

the velocity of the transverse acoustic waves polarized along $[0\bar{1}1]$ is larger than for $[\bar{2}33]$ polarization. This is in agreement with the corresponding bulk velocities of sound (see Table I). The QT and QL folded acoustic phonon doublets are of similar strength for the $z(x'x')\bar{z}$ polarization, whereas in the $z(y'y')\bar{z}$ polarization the QT-mode intensity is nearly half that of the QL mode.

The Rayleigh ratio σ_B^j (i.e., the scattering efficiency) of the jth acoustic mode $(j = T,\ QT,\ QL)$ with velocity v_j is[14]

$$\sigma_B^j = \frac{kT\pi^2}{2\lambda_s^4\rho v_j^2}[\hat{e}_s R^j \hat{e}_0]^2\frac{n_s}{n_0},\qquad(10)$$

where λ_s is the wavelength of the scattered light, T is the temperature, R^j is the Brillouin tensor [see Eqs. (5), (6), and (7)] and $\hat{e}_0$ and $\hat{e}_s$ are the unit vectors of the incident and scattered light, respectively. For the case of $z(x'x')\bar{z}$ polarizations this leads to

$$\frac{\sigma_B^{QT}}{\sigma_B^{QL}} = \left|\frac{a}{b}\right|^2\left[\frac{v_{QL}}{v_{QT}}\right]^2\qquad(11)$$

with a, b evaluated from Eqs. (8), using instead of p_{ij} the difference in the corresponding elastic-optic constants of the two constituent materials. Whereas these constants (real and imaginary part) have been measured recently for GaAs,[15] those of AlAs are unknown. Therefore we calculated the Rayleigh ratios using the elasto-optic constants of GaP,[16,17] which should be very similiar to those of AlAs in view of the fact that the band structures of both materials are nearly the same. Indeed, this approach improves the agreement of experimental and calculated values and will be used in the following. The p_{ij} of GaAs and GaP for 4579 and 5145 Å are compiled in Table III.

With the relation between the velocities of sound of the superlattice and the frequency splitting of the doublets [Eq. (9)] this yields

$$\frac{\sigma_B^{QT}}{\sigma_B^{QL}} \sim \left|\frac{a}{b}\right|^2\left[\frac{\Delta\omega_{QL}}{\Delta\omega_{QT}}\right]^2 = 1.32.\qquad(12)$$

Similarly, for the $z(y'y')\bar{z}$ polarizations results

$$\frac{\sigma_B^{QT}}{\sigma_B^{QL}} \sim \left|\frac{d}{e}\right|^2\left[\frac{\Delta\omega_{QL}}{\Delta\omega_{QT}}\right]^2 = 0.56.\qquad(13)$$

This is in good agreement with the findings of 1.4 and 0.4 in Fig. 2(a), respectively.

We show in Fig. 2(b) that the frequencies of the folded phonon doublets agree with predictions based on the continuum model. To investigate a possible influence of thickness fluctuations caused by the corrugation, we compared the linewidths of the folded acoustic phonons of this sample with a sample of identical thickness, but grown along [100]. As opposed to the confined optical phonons,[18] no pronounced effect of the corrugation can be detected for acoustic phonons. This is due to the fact that the acoustic waves are only sensitive to the average period of the superlattice.

Figure 3 shows the spectra from the SL with the largest period, (66/61) Å, measured with a SOPRA 2.12-m monochromator to achieve better resolution of the different phonon branches. In this figure, besides first order doublets, two weak features at 22.5 and 25.6 cm^{-1} can be observed. We assign them to the third-order QT doublet because of the agreement with the calculated frequencies (upper part of Fig. 3). In addition, also the QT-, QL-, and T-Brillouin modes (labeled B_{QT}, B_{QL}, and B_T) are observed. The relative intensities of the folded phonons with respect to the Brillouin mode can be used, in principle, to determine the ratio of the elasto-optic constants of GaAs and AlAs,[13,19–21] using the expression given in Ref. 13 or the more exact one of Ref. 19. In our case, this yields the linear combinations of the elasto-optic constants contributing to the scattering intensities in the different polarization geometries. The accuracy obtained by applying this procedure is, however, very poor because of the small values of the elasto-optic constants of AlAs in our frequency range. Therefore, we use another approach and calculate expected intensity ratios using, as mentioned earlier, the elasto-optic constants of GaP in lieu of AlAs. In Table IV we give the experimental and calculated values for the relative intensities as the average of the $m = -1$ and the $m = +1$ modes. To account for the difference between GaP and AlAs we assume that their elasto-optic constants may differ by less than 10%. This yields an error of $\approx 1\%$ for the calculated relative intensities. The measured and calculated values of all three intensity ratios agree then within the experimental uncertainty. This confirms that the elasto-optic constants of GaP can be used instead of those of AlAs in the region below the direct gap E_0. The experimental values

TABLE III. Elasto-optic constants of GaAs (Ref. 14) and GaP (Refs. 16 and 17) defined as derivatives of the dielectric function (not its inverse) vs strain.

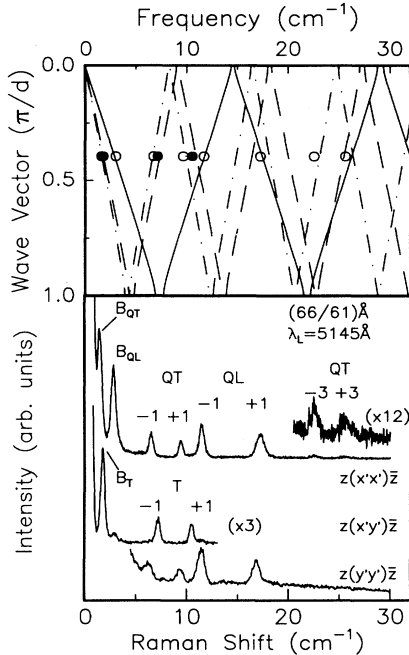| Material	λ_L (Å)	Elasto-optic constants		
		p_{11}	p_{12}	p_{44}
GaAs	4579	$115.7 - i\ 35.6$	$40.7 + i\ 199.1$	$199.7 + i\ 27.4$
	5145	$67.2 - i\ 28.7$	$11.7 + i\ 105.0$	$155.9 - i\ 10.7$
GaP	4579	30.4	28.3	-5.8
	5145	13.9	19.9	-11.1

FIG. 3. Raman spectra of the (66/61)-Å superlattice, measured with a SOPRA double monochromator. In this case, the Brillouin lines of all three branches, B_T, B_{QT}, B_{QL}, as well as the third-order QT doublet can be observed.

TABLE IV. Ratio of the intensities of the folded acoustic phonons to those of the corresponding Brillouin modes. The theoretical values were calculated using Eq. (60) of Ref. 19 and the elasto-optic constants of GaAs (Ref. 15) and GaP (Refs. 16 and 17) (in lieu of AlAs). Both measured and calculated values represent the average of the $m = -1$ and $m = +1$ modes.

| | I_m/I_B | |
Acoustic mode	Experiment	Theory
T	0.325 ± 0.050	0.361 ± 0.004
QT	0.360 ± 0.054	0.341 ± 0.003
QL	0.360 ± 0.054	0.380 ± 0.004

of Table IV are taken from the spectra with $z(x'x')\bar{z}$ and $z(x'y')\bar{z}$ polarizations. In $z(y'y')\bar{z}$ polarizations Rayleigh scattering is stronger and the Brillouin mode could not be observed. This different behavior for both polarizations is presumably caused by the different orientation of the sample corrugation[6] with respect to the plane of incidence. The Rayleigh ratios $\sigma_B^{QT}/\sigma_B^{QL}$ determined from

$z(x'x')\bar{z}$ $[z(y'y')\bar{z}]$ polarizations are 0.8 (0.35) as compared to 1.05 (0.33) obtained using Eqs. (11)–(13).

IV. CONCLUSION

In conclusion, we have observed the folded transverse (T), quasitransverse (QT), and quasilongitudinal (QL) acoustic-phonon modes in the case of (311)-oriented GaAs/AlAs superlattices. The measured frequencies of these modes compare well with calculations based on the elastic continuum model. In the sample with the largest period we have also measured the Brillouin modes of all three acoustic branches and have shown that the relative intensities of the folded phonons to the corresponding Brillouin modes can be described by the elasto-optic constants of GaAs and GaP.

ACKNOWLEDGMENTS

*Permanent address: Paul-Drude-Institut für Festkörperelektronik, O-1086 Berlin, Federal Republic of Germany.

[1] Z.V. Popović, M. Cardona, E. Richter, D. Strauch, L. Tapfer, and K. Ploog, Phys. Rev. B **40**, 1207 (1989).

[2] Z.V. Popović, M. Cardona, E. Richter, D. Strauch, L. Tapfer, and K. Ploog, Phys. Rev. B **40**, 3040 (1989).

[3] Z.V. Popović, M. Cardona, E. Richter, D. Strauch, L. Tapfer, and K. Ploog, Phys. Rev. B **41**, 5904 (1990).

[4] Z.V. Popović, M. Cardona, E. Richter, D. Strauch, L. Tapfer, and K. Ploog, Phys. Rev. B **43**, 4925 (1991).

[5] T. Hajakawa, K. Takahashi, M. Kondo, T. Sujama, S. Yamamoto, and T. Hijikata, Phys. Rev. Lett. **60**, 349 (1989).

[6] R. Nötzel, N.N. Ledentsov, L. Däweritz, K. Ploog, and M. Hohenstein, Phys. Rev. B **45**, 3507 (1992).

[7] S.H. Kwok, R. Merlin, W.Q. Li, and P.K. Bhattacharya, J. Appl. Phys. **72**, 285 (1992).

[8] B. Jusserand and M. Cardona, in Light Scattering in Solids V, edited by G. Güntherodt and M. Cardona (Springer, Heidelberg, 1989), p. 49.

[9] Z.V. Popović, J. Trodahl, M. Cardona, E. Richter, D. Strauch, and K. Ploog, Phys. Rev. B **40**, 1202 (1989).

[10] R. Nötzel, L. Däweritz, and K. Ploog, Phys. Rev. B **46**, 4736 (1992).

[11] B.A. Auld, Acoustic Fields and Waves in Solids (Wiley, New York, 1973), Vol. 1, p. 191.

[12] Data in Science and Technology; Semiconductors, Group IV Elements and III-V Compounds, edited by O. Madelung (Springer, Berlin, 1991), p. 105.

[13] C. Colvard, T.A. Gant, M.V. Klein, R. Merlin, R. Fisher, H. Morkoc, and A.C. Gossard, Phys. Rev. B **31**, 2080 (1985).

[14] H.Z. Cummins and P.E. Schoen, in Laser Handbook, edited by F.T. Arechi and E.O. Schulz-Dubois (North-Holland, Amsterdam, 1972), p. 1029.

[15] P. Etchegoin, J. Kircher, M. Cardona, C. Grein, and E. Bustarret, Phys. Rev. B **46**, 15 139 (1992).

[16] F. Canal, M. Grimsditch, and M. Cardona, Solid State Commun. **29**, 523 (1979).

[17] K. Strössner, S. Ves, and M. Cardona, Phys. Rev. B **32**,

6614 (1985).

[18] A. J. Shields, R. Nötzel, M. Cardona, L. Däweritz, and K. Ploog, Appl. Phys. Lett. **60**, 2537 (1992).

[19] J. He, B. Djafari-Rouhani, and J. Sapriel, Phys. Rev. B **37**, 4086 (1988).

[20] J. Sapriel, J. He, B. Djafari-Rouhani, R. Azoulay, and F. Mollot, Phys. Rev. B **37**, 4099 (1988).

[21] J. He, J. Sapriel, and H. Brugger, Phys. Rev. B **39**, 5919 (1989).